Journal of Statistical Physics, Vol. 70, Nos. 5/6, 1993

Exact Solution of the Discrete (1 + 1)-Dimensional SOS Model with Field and Surface Interactions

Aleksander L. Owczarek[1] **and Thomas Prellberg**[1]

Received July 15, 1992

We present the solution of a linear solid-on-solid (SOS) model. Configurations are partially directed walks on a two-dimensional square lattice and we include a linear surface tension, a magnetic field, and surface interaction terms in the Hamiltonian. There is a wetting transition at zero field and, as expected, the behavior is similar to a continuous model solved previously. The solution is in terms of q-series most closely related to the q-hypergeometric functions ${}_1\phi_1$.

KEY WORDS: Wetting transition; SOS model; directed walk; exact solution; q-series.

1. INTRODUCTION

In the study of the statistical mechanics of fluctuating interfaces in two dimensions the solid-on-solid (SOS) model has proved invaluable as a tractable though nevertheless effective approximation.[1,2] The SOS model arose from the consideration of the boundary between oppositely magnetized phases in the Ising model[3] at low temperatures and is now considered to be useful for describing the salient features of a wide variety of interfacial phenomena.[4–8] The approximation inherent in the SOS formulation of a phase boundary, that of no overhangs, implies that the configurations considered are simply those of *partially directed self-avoiding walks* (PDSAW). This relates the SOS model to problems in polymer physics.

Exact solutions in statistical mechanics are now viewed as an immensely important area of mathematical physics[9] where many results and techniques have proven to be widely applicable. Here we present the exact solution of the SOS model with a magnetic field and boundary potential in

[1] Department of Mathematics, University of Melbourne, Parkville, Victoria 3052, Australia.

0022-4715/93/0300-1175$07.00/0

addition to the usual linear surface tension. A generalized or grand partition function is found to be expressible in terms of q-series. We point out that q-series have played an important role in the solution of the more complex vertex and ABF-type models and these series are in general related to θ functions.[9] Our q-series, which has occurred previously in work on algebraic languages,[11] can be viewed as a q-generalization of Bessel functions, different from those defined classically.[10] The associated PDSAW problem is that of enumerating walks according to perimeter, area under the walk, and number of contacts with a wall. The interactions chosen lead naturally to the consideration of the critical phenomena in terms of critical and complete wetting transitions. These transitions are indeed there and the critical behavior is similar to a previously studied semicontinuum model where the solution is expressed in terms of Bessel functions.[12]

The SOS model we analyze is defined as follows. Consider a two-dimensional square lattice in a half-plane. For each column i of the surface a bond is placed on the horizontal link at height r_i and successive bonds are joined by vertical bonds to form a PDSAW. The configurations are given the energy

$$-\beta E = -K\sum_i |r_i - r_{i-1}| - H\sum_i r_i + b\sum_i \delta_{r_i,0} \tag{1}$$

Many aspects of several variants and subcases have been considered previously. The added restriction that $|\Delta r_i| = |r_i - r_{i-1}| \leqslant 1$, giving the *restricted* SOS (RSOS) model, has been extensively studied, especially with $H=0$,[2, 13] and considered[14] for several types of external potential. Without magnetic field the unrestricted model has also been investigated.[13, 15–18] Both variants have been considered, utilizing a different thermodynamic ensemble, as models for polymers in solution, since the finite configurations are PDSAW.[2, 19] Recently[20] an RSOS model with $H=0$ but a rigidity term dependent on $|\Delta r_i - \Delta r_{i-1}|$ has been considered as a model of semiflexible polymers such as DNA. Models in which the surface tension term depends on some integer power of $|\Delta r_i|$ larger than one have proven far more difficult to elucidate. Most relevant to this paper is the previous consideration[12] of the above SOS model in the limit when the vertical lattice spacing is taken to zero and hence the r_i are allowed to assume all positive real values. The full model has been analyzed using transfer integral techniques and the partition function is expressible in terms of Bessel functions. The phase diagram contains a wetting transition at finite temperature T_w for zero field and complete wetting occurs taking the limit $H \to 0$ for $T \geqslant T_w$. It is believed that the discrete model would have the same critical behavior, since renormalization group theory predicts a single set of exponents for critical and complete wetting[4] in systems with short-range forces, and we confirm this expectation.

We solve the SOS model defined above using a method first explained by Temperley.[21] This requires the deduction of a set of recurrence equations (12) relating an infinite set of generating functions. These take on two forms, the first being a set of *sum* equations (12) and the second *difference* equations (20). These are the discrete analogues of the integral and differential equations, respectively, that occur in the analysis of the continuous model. These equations are similar to the eigenvalue equations set up in a transfer matrix formulation, but have the advantage that one does not need to sum over the eigenvalues, after solving the equations, to find an expression for the generating function. We extend these methods by pointing out that they are equivalent to solving a functional equation (47) for the generating function. The functional equation puts the solution of the discrete and continuous models on the same footing. A second functional equation allows the solution to be written as a continued-fraction expansion. Intriguingly, the two functional equations are related to different geometric protocols. In general, continued-fraction expansions are useful because of the powerful theorems that can be brought to bear concerning the analytic structure of the solution.[22] Here they also facilitate numerical calculation and the derivation of exponents. Another point we make is that the solution is related to a variety of walk and polygon problems by the method of necklacing. In particular, the problem of enumerating bar-graph polygons by area and perimeter is enough to provide a solution to the SOS model.

The layout of the paper is as follows. In Section 2 we define precisely the partition and generating function for the SOS model. In Section 3 we set up the recurrence relations and show that other generating functions of interest can be found by simple concatenation arguments. The solution encapsulated in Eqs. (27), (38), (42), and (44) is set out in Section 4, the functional equations are discussed in Section 5, and the discussion of the singularity structure and phase diagram can be found in Section 6. We end with some comments on the wider relevance of this work.

2. SOS PARTITION FUNCTION

The fundamental quantity of interest is the partition function in the large-walk limit. We now define this more carefully. The partition function for the SOS walks[2] of length N fixed at both ends is given by

$$Z_1(r_0; r_1) = \exp[-\beta E(r_0; r_1)] \tag{2}$$

[2] SOS walks are PDSAWs that have been ascribed a weight according to the SOS Hamiltonian.

and

$$Z_N(r_0; r_N) = \sum_{r_1=0}^{\infty} \cdots \sum_{r_{N-1}=0}^{\infty} \exp[-\beta E(r_0; r_1, ..., r_N)], \qquad N = 2, 3, ... \tag{3}$$

where

$$-\beta E(r_0; r_1, ..., r_N) = -K \sum_{i=1}^{N} |r_i - r_{i-1}| - H \sum_{i=1}^{N} r_i + b \sum_{i=1}^{N} \delta_{r_i,0} \tag{4}$$

It is standard to define

$$Z_N = \sum_{r_N=0}^{\infty} Z_N(0; r_N), \qquad N = 1, 2, ... \tag{5}$$

so that Z_N is the partition function for our SOS interface fixed at one end and the other end allowed to be free. We define

$$y = \exp(-K), \qquad q = \exp(-H), \qquad \kappa = \exp(b) \tag{6}$$

so y is a temperature-like, q a magnetic field-like, and κ a binding energy-like variable, and write

$$Z_N = Z_N(y, q, \kappa) \tag{7}$$

The free energy is then

$$-\beta f(y, q, \kappa) = \lim_{N \to \infty} \frac{1}{N} \log Z_N(y, q, \kappa) \tag{8}$$

Define the generalized (grand canonical) partition function, or simply generating function, as

$$G^{(1)}(x, y, q, \kappa) = \sum_{N=1}^{\infty} x^N Z_N(y, q, \kappa) \tag{9}$$

Thus, the radius of convergence $x_c(y, q, \kappa)$ of $G^{(1)}(x, y, q, \kappa)$ with respect to the series expansion in x can be identified as $\exp(\beta f(y, q, \kappa))$; hence

$$f(y, q, \kappa) = kT \log x_c(y, q, \kappa) \tag{10}$$

3. THE RECURRENCE RELATIONS

By considering SOS walks[3] (see Fig. 1) that finish with a horizontal step at height r, we define a generating function for those walks as

$$G_r = \sum_{N=1}^{\infty} x^N Z_N(0; r) \tag{11}$$

[3] To be precise, SOS walks start at the surface and travel in either the horizontal or vertical direction and end with a horizontal step.

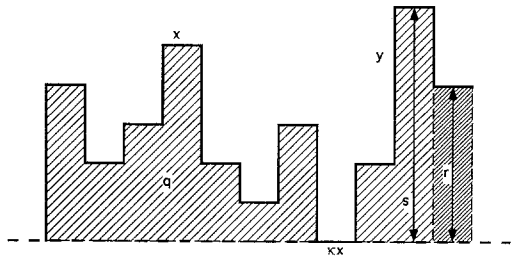

Fig. 1. A typical SOS configuration beginning on the surface and finishing at a height r with a horizontal step: each horizontal step is assigned a weight x, each vertical step a weight y, each unit of area (shaded) a weight q, and each step that touches the surface a weight κx. The picture also indicates how such a walk can be constructed out of a walk ending at a height s by adding a horizontal step at a height r, which multiplies its Boltzmann weight by $xy^{|r-s|}q^r$. This is the essential procedure in deriving Temperley's recurrence relation (12).

The observation of importance is that walks that end at height r are made of walks of all heights that finish one column to the left plus the extra vertical steps, one horizontal step, and area (field) weighting required to complete the walk. Taking account of walks that visit the surface just before the last column and walks that have just begun leads to the following recursion relation:

$$G_r = x[1+\delta_{r,0}(\kappa-1)]\, q^r \left(y^r + \sum_{s=0}^{\infty} y^{|r-s|} G_s \right), \qquad r=0,\ 1,\ldots \tag{12}$$

This is the *sum* equation mentioned in the introduction and its derivation is a fundamental step in the method of Temperley. We now show how knowledge of the G_r allows the calculation of several generating functions of interest, including $G^{(1)}(x, y, q, \kappa)$. Defining

$$\mathcal{G}(x, y, q, \kappa; \mu) = \sum_{r=0}^{\infty} \mu^r G_r \tag{13}$$

we obtain the generating function for SOS walks ending on the surface as

$$G^{(11)}(x, y, q, \kappa) = \sum_{N=1}^{\infty} x^N Z_N(0;0) = \kappa x[1+\mathcal{G}(x, y, q, \kappa; y)] \tag{14}$$

whereas the generating function for SOS walks ending at arbitrary height (and by symmetry one starting with a horizontal step at an arbitrary height and finishing at the surface without a step) as defined in (9) is given as

$$G^{(1)}(x, y, q, \kappa) = \mathcal{G}(x, y, q, \kappa; 1) \tag{15}$$

Generally, walks starting at an arbitrary height that touch the surface at least once can be written as the concatenation of two SOS walks (possibly

of zero length), one of them not having any contacts with the surface except for its starting point ($\kappa = 0$), i.e.,

$$[1 + \mathcal{G}(x, y, q, \kappa, 1)]\, \kappa x [1 + \mathcal{G}(x, y, q, 0; 1)] \tag{16}$$

Similarly, the sum of all walks whose minimal distance to the surface is equal to r can be written as

$$[1 + \mathcal{G}(xq^r, y, q, 1; 1)]\, xq^r [1 + \mathcal{G}(xq^r, y, q, 0; 1)] \tag{17}$$

so that the sum of all walks which start and end with horizontal steps is given by

$$\begin{aligned}&[1 + \mathcal{G}(x, y, q; \kappa; 1)]\, \kappa x [1 + \mathcal{G}(x, y, q, 0; 1)] \\ &\quad + \sum_{r=1}^{\infty} [1 + \mathcal{G}(xq^r, y, q, 1; 1)]\, xq^r [1 + \mathcal{G}(xq^r, y, q, 0; 1)]\end{aligned} \tag{18}$$

We remark that this sum is only meaningful for $|q| < 1$.

4. SOLVING THE RECURRENCE RELATIONS

Starting with (12), we will now derive a homogeneous second-order difference equation which we can solve using an ansatz from ref. 2. Using the scaling behavior of the solutions, we can eliminate one of the two linearly independent solutions. We conclude by writing the general solution of (12) as an expression involving the quotient of two q-hypergeometric functions.

Taking differences in (12), we first eliminate the inhomogeneous term,

$$G_{r+1} - qyG_r = x(1 - y^2) \left(\frac{q}{y}\right)^{r+1} \sum_{s=0}^{r} y^s G_s, \qquad r = 1, 2, \ldots \tag{19}$$

Upon taking differences a second time, we are left with

$$(G_{r+2} - qyG_{r+1}) - \frac{q}{y}(G_{r+1} - qyG_r) = x\left(qy - \frac{q}{y}\right) q^{r+1} G_{r+1}, \qquad r = 1, 2, \ldots \tag{20}$$

This is the *difference* equation mentioned in the introduction. If the right-hand side of this equation were zero, it would be a homogeneous difference equation with constant coefficients. Its characteristic polynomial $P(\lambda)$ is

$$P(\lambda) = (\lambda - qy)\left(\lambda - \frac{q}{y}\right) \tag{21}$$

and the solution is given by $G_r = A_1(qy)^r + A_2(q/y)^r$.

This motivates the ansatz[2]

$$G_r = \lambda^r \sum_{n=0}^{\infty} c_n(q) q^{nr}, \qquad r = 1, 2, \ldots \tag{22}$$

which inserting into (20) gives

$$P(\lambda) c_0 + \sum_{n=1}^{\infty} q^{nr} \left[P(\lambda q^n) c_n + x \left(\frac{q}{y} - qy \right) \lambda q^n c_{n-1} \right] = 0 \tag{23}$$

This equation is solved by

$$P(\lambda) = 0, \qquad \text{i.e.,} \quad \lambda_1 = qy \quad \text{and} \quad \lambda_2 = \frac{q}{y} \tag{24}$$

and, choosing $c_0 = 1$,

$$c_n = \prod_{m=1}^{n} x \frac{(qy - q/y)\, \lambda q^m}{P(\lambda q^m)} = \frac{[x(y - 1/y)\lambda]^n\, q^{\binom{n}{2}}}{(\lambda/y; q)_n\, (\lambda y; q)_n} \tag{25}$$

where we have used the standard abbreviation

$$(x; q)_n = \prod_{m=1}^{n} (1 - x q^{m-1}) \tag{26}$$

Defining

$$H(x, q, t) = \sum_{n=0}^{\infty} \frac{q^{\binom{n}{2}} (-t)^n}{(x; q)_n\, (q; q)_n} \tag{27}$$

we now can write the general solution of (20) as

$$\begin{aligned} G_r = {} & A_1 (qy)^r\, H\left(qy^2, q, x \left(\frac{1}{y} - y \right) qy q^r \right) \\ & + A_2 \left(\frac{q}{y} \right)^r H\left(\frac{q}{y^2}, q, x \left(\frac{1}{y} - y \right) \frac{q}{y} q^r \right) \end{aligned} \tag{28}$$

As an aside, we note that the function H is directly related to a basic hypergeometric function[10]

$$H(x, q, t) = {}_1\phi_1(0, x; q, t) \tag{29}$$

which can be seen to be a limiting function of ${}_2\phi_1$ and that is the q-deformation of the more familiar hypergeometric function ${}_2F_1$. Analogously, the

function H can be understood (apart from some normalizing factors and seen by taking the limit $q \to 1$) as a q-generalization of Bessel functions. Furthermore, formally taking the continuum limit vertically transforms (using, in addition, various variable substitutions) Eq. (20) into Bessel's differential equation. Therefore, the solution above is also related via this second limit to Bessel functions.

Returning to the analysis, we see that, for $|q|<1$, $H(x, q, tq^r)$ is uniformly bounded in r, so that we can write

$$|G_r| \leqslant \text{const} \cdot \left[(qy)^r + \left(\frac{q}{y}\right)^r \right] \tag{30}$$

This we insert into (12) and, assuming $0<q<y^2<1$, we get

$$\begin{aligned} |G_r| &\leqslant \text{const} \cdot q^r \left[y^r + \sum_{s=0}^{r-1} y^{r-s} \left(\frac{q}{y}\right)^s + \sum_{s=r}^{\infty} y^{s-r} \left(\frac{q}{y}\right)^s \right] \\ &\leqslant \text{const} \cdot (qy)^r \left[1 + \left(\frac{q}{y^2}\right)^r \right] \leqslant \text{const} \cdot (qy)^r \end{aligned} \tag{31}$$

As $H(x, q, tq^r) \to 1$ for $r \to \infty$, we see that in fact $A_2 = 0$. Using the appropriate boundary conditions for G_0 and G_1 from (12), we can determine the constant A_1.

Once we have the right ansatz, though, another way is more convenient. We write in analogy to the above

$$G_r = [1 + \delta_{r,0}(\kappa - 1)] \lambda^r \sum_{n=0}^{\infty} c_n(q)[q^r]^n, \qquad r = 0, 1, \ldots \tag{32}$$

where we accommodate the particular boundary conditions of our problem. Substituting this ansatz, we have

$$\begin{aligned} \frac{1}{x} \lambda^r \sum_{n=0}^{\infty} c_n q^{nr} &= (qy)^r + (qy)^r \sum_{n=0}^{\infty} c_n \left(\frac{1}{1 - \lambda q^n / y} + \kappa - 1 \right) \\ &\quad + \lambda^r \sum_{n=1}^{\infty} c_{n-1} q^{nr} \left(\frac{1}{1 - \lambda q^{n-1} y} - \frac{1}{1 - \lambda q^{n-1}/y} \right) \end{aligned} \tag{33}$$

so that, again, $\lambda = qy$ and furthermore

$$c_n = -\frac{x(1-y^2)q^n}{(1-q^n)(1-y^2q^n)} c_{n-1} = \frac{[-x(1-y^2)q]^n q^{\binom{n}{2}}}{(q;q)_n (qy^2;q)_n} c_0 \tag{34}$$

with normalization

$$\frac{1}{x}c_0 = 1 + \sum_{n=0}^{\infty}\left(\frac{1}{1-q^{n+1}} + \kappa - 1\right)c_n \tag{35}$$

This implies

$$\frac{1}{c_0} = \frac{1}{x}H(y^2, q, x(1-y^2)) - (\kappa-1)\,H(qy^2, q, x(1-y^2)q) \tag{36}$$

so that

$$G_r = [1+\delta_{r,0}(\kappa-1)]\,x(qy)^r \times \frac{H(qy^2, q, x(1-y^2)q^{1+r})}{H(y^2, q, x(1-y^2)) - (\kappa-1)\,xH(qy^2, q, x(1-y^2)q)} \tag{37}$$

Defining the functions

$$g_r(x, y, q) = H(qy^2, q, x(1-y^2)q^{1+r}) \tag{38}$$

and

$$h(x, y, q) = H(y^2, q, x(1-y^2)) = (1-y^2)^{-1}\,[(1-x-xy^2)\,g_0 - y^2 g_1] \tag{39}$$

we can write simply

$$G_r = [1+\delta_{r,0}(\kappa-1)]\,x(qy)^r\,\frac{g_r}{h-(\kappa-1)xg_0} \tag{40}$$

so that we have

$$\mathcal{G}(x, y, q, \kappa; \mu) = x\,\frac{g(\mu) + (\kappa-1)\,g_0}{h-(\kappa-1)xg_0} \tag{41}$$

where

$$g(\mu) = \sum_{r=0}^{\infty}(\mu qy)^r\,g_r(x, y, q) \tag{42}$$

$$= \sum_{n=0}^{\infty}\frac{[-x(1-y^2)q]^n\,q^{\binom{n}{2}}}{(q;q)_n\,(qy^2;q)_n}\,\frac{1}{1-\mu yq^{1+n}} \tag{43}$$

For $|q|<1$, the only effect of the extra factor $(1-\mu yq^{1+n})^{-1}$ in the sum, which differentiates this expression from a q-Bessel function, is the introduction of additional poles at $\mu yq^{1+n}=1$. Apart from these poles, the

domain of convergence and thus the locus of singularities of $\mathscr{G}(\mu)$ are independent of μ. Specifying $\mu = 1$, we get

$$G^{(1)}(x, y, q, \kappa) = x \frac{g(1) + (\kappa - 1) g_0}{h - (\kappa - 1) x g_0} \tag{44}$$

The function $g(y)$ can be written in terms of q-Bessel functions, leading to

$$G^{(11)}(x, y, q, \kappa) = \kappa x \frac{g_0}{h - (\kappa - 1) x g_0} \tag{45}$$

The solutions (44) and (45) have been written in a way suggestive of the singularity structure needed to discuss the phase diagram. To this end, we notice that the generating functions diverge when, implicitly,

$$x = \frac{1}{\kappa - 1} \frac{h(x, y, q)}{g_0(x, y, q)} = \frac{1}{\kappa - 1} \frac{H(y^2, q, x(1 - y^2))}{H(qy^2, q, x(1 - y^2)q)} \tag{46}$$

and that this depends analytically on κ for $q < 1$. So the behavior of the ratio h/g_0 as well as $g(1)/g_0$ has to be considered to completely characterize the singularity structure. This can be done by making considerations similar to those of ref. 23. The results of this analysis necessary for the phase diagram will be discussed in Section 6.

5. FUNCTIONAL EQUATIONS

In this section we outline alternative solution procedures that utilize functional equations. In the field of exact solutions[9] functional equation techniques have proven to be of importance and so their relationship to other methods in a model such as this is of some interest. Also, as we shall see, there are two different ways of writing down functional equations, related to different geometrical approaches. One of these approaches leads to a series expansion, whereas the other leads to a continued-fraction expansion of the generating function. So, in addition to providing an additional route to the solution, they facilitate mathematical insights into the problem.

In extension of the Temperley method, the recurrence relation (12) implies a functional equation for $\mathscr{G}(\mu) = \sum_{r=0}^{\infty} \mu^r G_r$:

$$\frac{1}{x} \mathscr{G}(\mu) = (\kappa - 1) + \frac{1}{1 - \mu q y} + \left[(\kappa - 1) + \frac{1}{1 - \mu q / y} \right] \mathscr{G}(y) + \left(\frac{1}{1 - \mu q y} - \frac{1}{1 - \mu q / y} \right) \mathscr{G}(\mu q) \tag{47}$$

This functional equation has a counterpart of similar form for the semi-continuous model:

$$\frac{1}{x}\mathcal{G}(\mu)=(\kappa-1)+\frac{1}{-\log(\mu q y)}+\left[(\kappa-1)+\frac{1}{-\log(\mu q/y)}\right]\mathcal{G}(y)$$
$$+\left(\frac{1}{-\log(\mu q y)}-\frac{1}{-\log(\mu q/y)}\right)\mathcal{G}(\mu q) \tag{48}$$

which illustrates the equal complexity of the two models.

Iteration of the first equation is another way of deriving the results of the previous section in the form of the same series expansions. Substituting $q^n\mu$ for μ and multiplying with

$$\pi(n)=x^n\prod_{m=0}^{n-1}\left(\frac{1}{1-\mu q^m y}-\frac{1}{1-\mu q^m/y}\right) \tag{49}$$

gives

$$\frac{1}{x}\left[\pi(n)\,\mathcal{G}(\mu q^n)-\pi(n+1)\,\mathcal{G}(\mu q^{n+1})\right]$$
$$=\pi(n)\left\{(\kappa-1)+\frac{1}{1-\mu q^{n+1}y}+\left[(\kappa-1)+\frac{1}{1-\mu q^{n+1}/y}\right]\mathcal{G}(y)\right\} \tag{50}$$

Provided that $\lim_{n\to\infty}\pi(n)\,\mathcal{G}(\mu q^n)=0$, we now can sum over n and get

$$\mathcal{G}(\mu)=x\sum_{n=0}^{\infty}\pi(n)\left\{(\kappa-1)+\frac{1}{1-\mu q^{n+1}y}\right.$$
$$\left.+\left[(\kappa-1)+\frac{1}{1-\mu q^{n+1}/y}\right]\mathcal{G}(y)\right\} \tag{51}$$

Inserting $\mu=y$ determines $\mathcal{G}(y)$ and the resulting expression can be checked to coincide with the results from the previous section, e.g., Eq. (41). An analogous argument leads to the solution of the continuous model.

However, an entirely different method based on a (recursive) necklacing argument enables us to derive a functional equation for the generating function. This procedure leads to a continued-fraction representation of the generating function.

Let $K(x, y, q)$ denote the generating function for either a walk which consists of a horizontal step or a walk which starts and ends on the surface without additional contacts and is followed by a horizontal step, i.e.,

$$K(x, y, q)=x[1+\mathcal{G}(x, y, q, 0; y)] \tag{52}$$

$K(x, y, q)$ is simply related to $G^{(11)}(x, y, q, 0)$ at $\kappa = 0$, as can be seen from (14). Thinking of the walks that contribute to $K(x, y, q)$, we can view $K(x, y, q)$ as the concatenation of copies of itself, which are shifted into the y direction by one vertical step, i.e., $K(qx, y, q)$. This leads, after some combinatorics, to an equation relating these two generating functions:

$$K(x, y, q) = \frac{1}{q}\left\{ y \sum_{n=1}^{\infty} [K(qx, y, q)]^n - yqx + qx \right\} \tag{53}$$

Summing, one obtains

$$K(x, y, q) = \left[x(1-y) - \frac{y}{q} \right] + \frac{y}{q} \frac{1}{1 - K(qx, y, q)} \tag{54}$$

or, expressed in terms of $\mathscr{G}(x, y, q, 0; y)$,

$$G(x, y, q, 0; y) = y \frac{qx + (1+qx)\, G(qx, y, q, 0; y)}{(1-qx) - qxG(qx, y, q, 0; y)} \tag{55}$$

The generating function $G^{(11)}$ (now for arbitrary κ) is given by

$$G^{(11)}(x, y, q, \kappa) = \sum_{n=1}^{\infty} \kappa [K(x, y, q)]^n = -1 + \frac{1}{1 - \kappa K(x, y, q)} \tag{56}$$

Iteration of Eq. (54) readily leads to a continued-fraction expansion for $K(x, y, q)$ and thus for $G^{(11)}$. Defining

$$a_n = 1 + \frac{y}{q} - xq^n(1-y), \qquad b_n = -\frac{y}{qa_n a_{n+1}} \tag{57}$$

we can write

$$1 - K(x, y, q) = a_0 - \cfrac{y/q}{a_1 - \cfrac{y/q}{a_2 - \cfrac{y/q}{a_3 - \cfrac{y/q}{a_4 - \cdots}}}} \tag{58}$$

$$= a_0 \left(1 + \cfrac{b_1}{1 + \cfrac{b_2}{1 + \cfrac{b_3}{1 + \cfrac{b_4}{1 + \cdots}}}}\right) \tag{59}$$

which certainly converges if $|b_n| \leqslant 1/4$, for all n.[22]

We note that another, more powerful continued-fraction expansion can be found by working directly with ratios of the q-Bessel function (that is, once the series solution has been found). Here, instead, we want to emphasize and contrast the geometric background of these two types of functional equations and the structure of their solutions. One advantage of the second functional equation is that it provides us with a protocol for the computation of the critical exponents. We observe that the computation of the generating functions on the line $q=1$ is a relatively simple matter, and, upon partial differentiation of Eqs. (54) and (56) and insertion of $q=1$, the various partial derivatives of $G^{(11)}$ with respect to its arguments can be readily computed. Investigation of their divergences and a scaling ansatz leads in turn to the computation of the critical exponents, the results of which are given in the next section. We will discuss these techniques in more detail in a further paper.[24]

6. SINGULARITY STRUCTURE AND PHASE DIAGRAM

To begin this discussion, we present the solution of the difference equations when $q=1$. The solution is easily obtained from (20) using the ansatz $G_r = CA^r$ in place of (22). After some elementary algebraic manipulations the generating function $G^{(1)}$ (we shall concentrate on this generating function here) is given by

$$G^{(1)}(x, y, 1, \kappa) = \frac{x(1-y^2)[(1-\kappa)A+\kappa]}{[1-x\kappa(1-y^2)-yA](1-A)} \tag{60}$$

where

$$2A = [(1/y+y)-x(1/y-y)] - [(1/y-y)^2(1+x^2)-2x(1/y^2-y^2)]^{1/2} \tag{61}$$

In our interface problem we consider the generating functions as power series in x and the coefficients are canonical partition functions of the interface problem. If, however, we set $x=y$, then the generating functions can be viewed as a power series in y where the coefficients are the partition functions of the related polymer model which are simply noninteracting PDSAWs above a "sticky" surface. Keeping this in mind, we can now check that our expression for the $G^{(1)}$ reproduces the previous results for that problem.[2]

The above expression for $G^{(1)}$ has two singularities in x: one at

$$x_c = x_b = \frac{\kappa - 1 - \kappa y^2}{\kappa(\kappa-1)(1-y^2)} \tag{62}$$

and also at

$$x_c = x_f = \frac{1-y}{1+y} \tag{63}$$

These can be checked by putting $x = y$ to produce the known results for the singularities in the polymer problem

$$\kappa(1-y^2)(1+y-\kappa y) = 1 \tag{64}$$

and

$$y\frac{(1+y)}{(1-y)} = 1 \tag{65}$$

It is enlightening to compare our expression (60) for the generating function with the expression obtained from the transfer matrix method,[19] where $x = y$. The transfer matrix method gives the generating function as an integral over a continuous spectrum plus a bound-state contribution. This method provides physical insights and allows the calculation of correlation functions, once the spectrum has been analyzed. Our technique, on the other hand, gives an immediate expression for the generating function which facilitates the calculation of exponents. This difference arises because the transfer matrix method requires the more subtle considerations of the mathematics of infinite-dimensional matrices and the subsequent normalization of eigenvectors.

Returning to our interface problem, we find that the two singularities are simultaneously achieved when

$$\kappa = \kappa_c = 1/(1-y) \tag{66}$$

When $\kappa < \kappa_c$ then $x_f < x_b$, so that for binding potentials less than a critical value the singularity does not depend on that potential. At fixed y, on varying κ, there is then a critical point κ_c. On closer examination it can be seen that this is just a critical wetting transition where the SOS interface binds to the surface on increasing κ. From analysis of the solution (44), for $q < 1$ the generating function has only one singularity that depends on κ. There is no longer a critical point and the interface is always bound to the surface. In Fig. 2 the radius of convergence $x_c(y, q, \kappa)$ of the generating function, and hence the free energy, is plotted for fixed $y = 1/2$ at various values of κ above, at, and below $\kappa_c = 2$. We can see that on taking the limit $q \to 1$ (that is, $H \to 0$) for $\kappa < \kappa_c$ there is a cusp singularity in the free energy surface that is the sign of the complete wetting transition. For $\kappa > \kappa_c$ no such transition exists. Setting $q = 1$, we plot in Fig. 3 the radius of

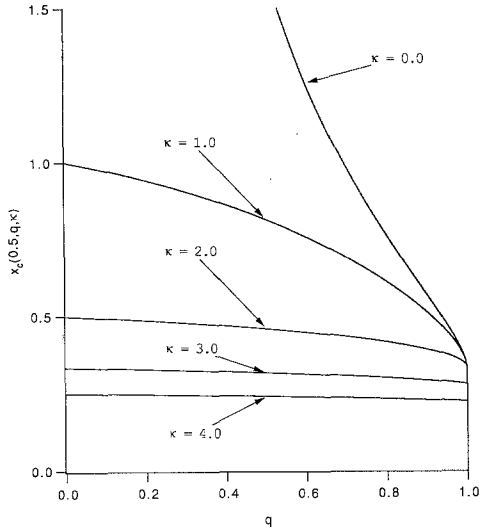

Fig. 2. The radius of convergence $x_c(y, q, \kappa)$ of $G^{(1)}(x, y, q, \kappa)$ at fixed $y = 1/2$ and for various values of $\kappa = 0.0$, 1.0, 2.0, 3.0, 4.0. The shape of the curves near $q = 1$ illustrates the difference in the system above and below $\kappa_c = 2$: below and including the critical κ_c, the curves approach the same value $x_c = 1/3$ with infinite slope (exponent 2/3); above κ_c the curves have finite slope at $q = 1$ and the limit varies with κ.

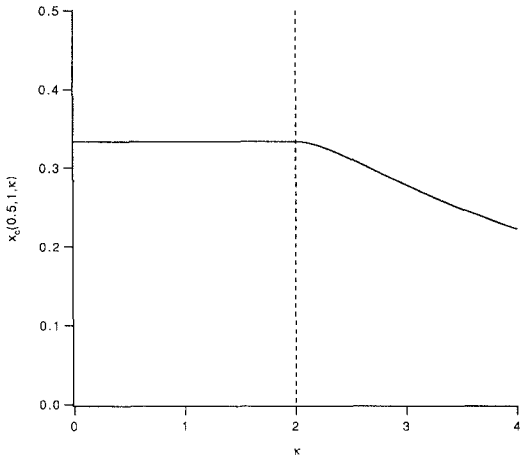

Fig. 3. The radius of convergence $x_c(y, q, \kappa)$ at fixed $y = 1/2$ and $q = 1$ plotted against κ. The radius of convergence is constant ($x_c = 1/3$) below $\kappa_c = 2.0$.

convergence of (60), again at fixed $y = 1/2$, to illustrate the critical wetting transition. These plots could equally well have been plotted against y for fixed κ producing the "binding" transition, described above, on decreasing y rather than increasing κ. The simple competition of temperature and binding potential is quantified by Eq. (66). To complete the picture, we give the phase diagram (Fig. 4), found from the singularities in the free energy, at fixed binding potential $\kappa = 2$ in the temperature–field (y–q) plane.

We are now in a position to discuss exponents. All the canonical or free energy exponents[4] and some of the grand canonical or generating function exponents[2] have been given explicitly (or at least implicitly) in previous works. The generating function $G^{(1)}$ always diverges on approaching its radius of convergence in this problem, although this is not necessarily the case in general. This ensures that the thermodynamic limit is taken, that is, $\langle N \rangle = \partial \log G / \partial \log x \to \infty$, and immediately tells us that the length of the interface is infinite. In fact, both the expected value of N and the length diverge linearly with the inverse distance to the radius of convergence surface, regardless of the temperature, magnetic, or binding fields. Exponents may then be calculated from the generating function.[2] Quantities (we use G to denote either generating function $G^{(1)}$ or $G^{(11)}$) that can be easily found are the average surface contact

$$\langle L_s \rangle = \frac{\partial \log G}{\partial \log \kappa} \tag{67}$$

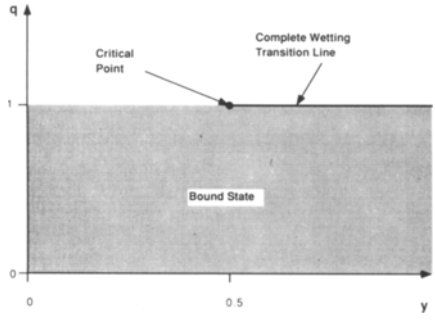

Fig. 4. The phase diagram (the singularities in the free energy rather than the generating function) at fixed $\kappa = 2.0$. There is a critical point at a temperature given by $y = 1/2$ and field $q = 1$ (that is, $H = 0$). For low temperatures $y < 1/2$ the interface is bound and no transition takes place on varying the field to zero, whereas for high temperatures $y > 1/2$ there is a line of complete wetting transitions, denoted by the line on the diagram.

and the average area under the interface

$$\langle A \rangle = \frac{\partial \log G}{\partial \log q} \tag{68}$$

These in turn give us exponents for the coverage

$$C(x, y, q, \kappa) = \frac{\langle L_s \rangle}{\langle N \rangle} \tag{69}$$

and the average distance of the interface to the wall

$$\langle L_d \rangle = \frac{\langle A \rangle}{\langle N \rangle} \tag{70}$$

The coverage in the limit $x \to x_c$, that is, $C(x_c, y, q, \kappa)$, can be seen to be an order parameter of the wetting transitions in addition to the standard one of the distance $\langle L_d \rangle$.

We first discuss the singularities in the generating function itself. We define the exponent γ by

$$G \sim (x_c - x)^{-\gamma} \tag{71}$$

for $(x_c - x)$ small. For $q < 1$ and $q = 1$ with $\kappa \geqslant \kappa_c$ there is a simple pole in the generating function and $\gamma^{(1)} = 1$. For $q = 1$ and $\kappa < \kappa_c$ the generating function has a square root singularity and $\gamma^{(1)} = 1/2$.

Next, one can consider the limit $q \to 1$ fixing $x = x_c(y, 1, \kappa)$ and $\kappa \leqslant \kappa_c$ to find

$$G^{(1)} \sim (1 - q)^{-1/3} \tag{72}$$

so that the grand canonical field crossover exponent is $\phi^q = 2/3$. This is confirmed by calculating the shape of the free energy surface for $\kappa \leqslant \kappa_c$ as $q \to 1$. This immediately gives the following result for the singularity in the canonical free energy at the complete wetting transition:

$$f_{\text{sing}} \sim H^{2/3} \tag{73}$$

that is, $\alpha_H = 4/3$.

Defining ν_s as the divergence exponent for the average number of contacts with the wall, we find that for $q < 1$, and $q = 1$ with $\kappa \geqslant \kappa_c$, $\nu_s = 1$, while for $\kappa < \kappa_c$, then $\langle L_s \rangle$ stays finite as $x \to x_c$. At the critical point, $\kappa = \kappa_c$ (and $q = 1$), $\nu_s = 1/2$, which implies that the coverage goes to zero with a square root singularity. From ref. 19 the coverage goes to zero

linearly as $\kappa \to \kappa_c^+$, which implies a grand canonical temperature or binding exponent $\phi^\kappa = 1/2$. (There is no change in crossing over from binding potential to temperature, as they are similar scaling fields at the critical wetting transition.) This exponent again agrees with the shape of the free energy surface, since

$$f_{\text{sing}} \sim (\kappa - \kappa_c)^2 \tag{74}$$

which gives $\alpha_\kappa = \alpha_T = 0$. We now immediately confirm the result that the temperature (or binding potential) to magnetic field crossover exponent[12] in the free energy is $1/3 = \phi^\kappa \phi^q$.

One can find exponents in all directions for the distance of the interface to the wall $\langle L_d \rangle$ by utilizing the crossover exponents and the known result[4] that

$$\langle L_d \rangle \sim (T_c - T)^{-1} \tag{75}$$

for zero field.

All the exponents can be either found directly from (60) or confirmed from (44) using the functional equations even though the theory of the asymptotics of basic hypergeometric functions has not been widely studied. By studying the continuous SOS model via our (suitably modified) method, all the exponents could have been calculated quite simply using the knowledge of the asymptotics of Bessel functions.

7. DISCUSSION

We have presented the exact solution of a much studied model of interfacial physics and have shown that the solutions of discrete models in this class are of the same level of difficulty as semicontinuum ones. However, as the solution (44) is expressed in terms of functions (27) that are somewhat recondite, it may seem more difficult. Since the two models have similar critical behavior, it implies that the asymptotics of q-series can sometimes be treated by approximation to ordinary special functions. We believe this observation may be of importance to the study of the asymptotics of q-series in general. We also have reiterated the importance of the method of Temperley, which can be extended to the semicontinuous model as an alternative to the transfer matrix method. We have shown that the solution can be found from either a difference/differential equation or a functional equation and can be written down in terms of a series or continued-fraction expansion. Using the functional equations, we have checked that the exponents are those that are expected of this problem and have given the three crossover exponents.

Another observation that can be made by considering SOS walks that do not touch the surface other than at the last step. Here one is equivalently considering the problem of enumerating bar-graph polygons (see Fig. 5) according to perimeter and area. Moreover, if one had considered this problem first, the generating function $G^{(11)}$ for the SOS walks could have been found by a necklacing argument.[6, 25] The generating function G_{bg} for these polygons is then given essentially by (13) with $\mu = y$ as

$$G_{bg}(x, y, q) = \mathscr{G}(x^2, y, q, 0; y) \tag{76}$$

and in turn gives via necklacing

$$G^{(11)}(x, y, q, \kappa) = \frac{\kappa x[1 + G_{bg}(x^{1/2}, y, q)]}{1 - \kappa x[1 + G_{bg}(x^{1/2}, y, q)]} \tag{77}$$

We remark also that the work of Zwanzig and Lauritzen[26, 27] and Nordholm[28] on a model of polymer crystallization (ZL) is related to the SOS model analyzed here with $\kappa = 1$ and the work of Abraham and Smith.[12] These authors considered, without identifying it, the $\kappa = 1$ transfer matrix/operator for the SOS model in a field. Even at $\kappa = 1$ the generating functions for the ZL and our SOS models are different, although related, because of the added restriction in the polymer model that requires the walks to "fold" at every turn.

Necklacing arguments are quite powerful and we show in another publication[24] that such an argument can be invoked also to relate the ZL model to the interacting PDSAW (IPDSAW) model,[23, 29] where one considers enumerating PDSAWs by length weighted with nearest-neighbor interactions on a fully infinite lattice. We caution the reader, however, that neither the IPDSAW nor the ZL model on semi-infinite lattices with a

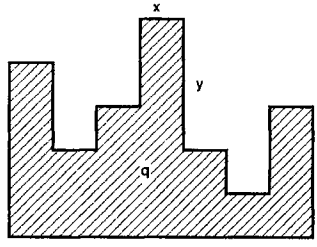

Fig. 5. A typical bar-graph polygon weighted by area $[q]$ (shaded), horizontal $[x]$, and vertical $[y]$ perimeters. These are essentially equivalent to SOS walks that begin and end on the surface without otherwise touching the surface apart from the fact that the bottom perimeter is also weighted. Hence, the polygons have the equivalent weight x^2 for each SOS walk horizontal step. The "no touching" constraint can be achieved by an infinite local repulsion, that is, $\kappa \to 0$.

surface interaction is related to the SOS problem of this paper, because the relationship between the two when $\kappa = 1$ requires a transformation to difference coordinates in the polymer problems.

ACKNOWLEDGMENTS

The authors thank R. Brak and A. J. Guttmann for enlightening discussions and are grateful to the Australian Research Council for financial support.

REFERENCES

1. G. Forgacs, R. Lipowsky, and Th. M. Nieuwenhuizen, *Phase Transitions and Critical Phenomena*, Vol. 14, C. Domb and J. L. Lebowitz, eds. (Academic Press, London, 1991).
2. V. Privman and N. M. Švrakić, *Lecture Notes in Physics*, No. 338 (Springer-Verlag, Berlin, 1989).
3. H. N. V. Temperley, *Proc. Camb. Phil. Soc.* **48**:638 (1952).
4. S. Dietrich, in *Phase Transitions and Critical Phenomena*, Vol. 12, C. Domb and J. L. Lebowitz, eds. (Academic Press, London, 1988).
5. N. M. Švrakić, V. Privman, and D. B. Abraham, *J. Stat. Phys.* **53**:1041 (1988).
6. M. E. Fisher, *J. Stat. Phys.* **34**:667 (1984).
7. D. B. Abraham, *Phys. Rev. Lett.* **50**:291 (1983).
8. D. B. Abraham and A. L. Owczarek, *Phys. Rev. Lett.* **64**:2595 (1990).
9. R. J. Baxter, *Exactly Solved Models in Statistical Mechanics* (Academic Press, London, 1982).
10. G. Gasper and M. Rahman, *Basic Hypergeometric Series* (Cambridge University Press, Cambridge, 1990).
11. M. P. Delest and J. M. Fedou, Enumeration of skew Ferrer diagrams, *Discrete Math.*, to appear.
12. D. B. Abraham and E. R. Smith, *J. Stat. Phys.* **43**:621 (1986).
13. S. T. Chui and J. D. Weeks, *Phys. Rev. B* **23**:2438 (1981).
14. V. Privman and N. M. Švrakić, *J. Stat. Phys.* **51**:1111 (1988).
15. J. T. Chalker, *J. Phys. A* **14**:2431 (1981).
16. T. W. Burkhardt, *J. Phys. A* **14**:L63 (1981).
17. H. Hilhorst and J. M. Van Leeuwin, *Physica* **107A**:319 (1981).
18. D. M. Kroll, *Z. Phys. B* **41**:345 (1981).
19. G. Forgacs, V. Privman, and H. L. Frisch, *J. Chem. Phys.* **90**:3339 (1989).
20. G. Forgacs, *J. Phys. A* **24**:1099 (1991).
21. H. N. V. Temperley, *Phys. Rev.* **103**:1 (1956).
22. H. S. Wall, *Analytic Theory of Continued Fractions* (van Nostrand, New York, 1948), p. 42.
23. R. Brak, A. Guttmann, and S. Whittington, *J. Phys. A* **25**:2437 (1992).
24. R. Brak, A. L. Owczarek, and T. Prellberg, in preparation.
25. D. B. Abraham and P. Duxbury, *J. Phys. A* **19**:385 (1986).
26. R. Zwanzig and J. I. Lauritzen, Jr., *J. Chem. Phys.* **48**:3351 (1968).
27. J. I. Lauritzen, Jr., and R. Zwanzig, *J. Chem. Phys.* **52**:3740 (1970).
28. K. Sture Nordholm, *J. Stat. Phys.* **9**:235 (1973).
29. P.-M. Binder, A. L. Owczarek, A. R. Veal, and J. M. Yeomans, *J. Phys. A* **23**:L975 (1990).